

# CNN-based Early Diagnosis of Breast Cancer with Variable Image Resolutions

Miraj Jara  
Department of Computer Science  
Southern Connecticut State University  
New Haven, CT, USA

Alaa Sheta  
Department of Computer Science  
Southern Connecticut State University  
New Haven, CT, USA

Walaa H. Elashmawi  
Department of Computer Science  
Misr International University  
Cairo, Egypt

## ABSTRACT

Breast cancer remains one of the most common and lethal forms of cancer globally. It impacts millions of women each year across various age groups, ethnicities, and socio-economic backgrounds. Early detection is critical for improving survival rates, as it allows for timely and less aggressive treatment options. While mammography has played a significant role in early diagnosis, it is limited by variability in interpretation and the potential for false positives and negatives. Recent deep learning (DL) advancements offer promising solutions for more accurate breast cancer detection. This paper presents a convolutional neural network (CNN) architecture designed to classify breast ultrasound images, distinguishing between malignant, benign, and normal tissues. The proposed CNN model was trained and tested on the Breast Ultrasound Images dataset with various image resolutions, including  $32 \times 32$ ,  $56 \times 56$ ,  $128 \times 128$ , and  $256 \times 256$  pixels. The results demonstrated that with an image resolution of  $256 \times 256$ , the CNN model achieved the highest accuracy of 99.87% and 83.49% in training and testing, respectively. The study emphasizes the potential of deep learning techniques in improving breast cancer detection accuracy and efficiency, ultimately leading to improved patient outcomes.

## Keywords

Breast Cancer, Deep Learning, Convolutional Neural Networks.

## 1. INTRODUCTION

Breast cancer is the foremost reason for cancer-related deaths among women. Millions of women are diagnosed with breast cancer yearly. Survival rates for breast cancer differ, and it is based on the quality of medical services in various regions of the world. For example, in North America, the survival rate is more than 80%; in Sweden and Japan, it is about 60%, which is lower in developing countries [27]. The low survival rate in developing countries is due to the absence of early detection programs and insufficient diagnostic and healthcare services. Thus, it is critical to utilize high technology such as Artificial Intelligence (AI), Machine Learning (ML), and DL methods to diagnose breast cancer even with low-quality images or images with less resolution. According to the World Health Organization, breast cancer continues to be a significant health concern worldwide, impacting millions of women annually. In 2022, breast cancer caused 670,000

deaths globally 2022, and roughly half of all cases occur in women with no specific risk factors other than sex and age. It manifests as an abnormal growth of cells within breast tissue, which can be classified into two primary categories: benign and malignant. Benign tumors, while non-cancerous, can still pose health risks and may require treatment to prevent complications. Malignant tumors, on the other hand, are cancerous and can invade nearby tissues or spread to different parts of the body, leading to more severe health outcomes[17].

Furthermore, The projected value of the global breast cancer market is estimated to reach around USD 49.2 billion by 2032, compared to USD 19.8 billion in 2022. This is a compound annual growth rate (CAGR) of 9.8% between 2022 and 2032, as illustrated in Figure 1. Over time, there has been an improvement in breast cancer survival rates. The breast cancer five-year survival rate in the United States is around 90%. The American Cancer Society advises women at medium risk, beginning at 40, to undergo yearly mammograms.

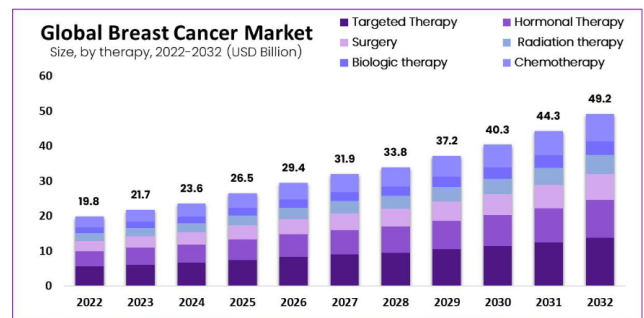


Fig. 1. Global Breast Cancer Market 2022-2032 [15]

In recent years, advancements in Deep Learning (DL) have revolutionized many real-life applications [2, 21, 7, 5] and also in medical image analysis, offering promising solutions for automated tumor classification[14]. Convolutional Neural Networks (CNNs) represent a compelling DL architecture for image classification tasks [13]. CNNs excel at automatically extracting relevant features from images through a series of convolutional and pooling layers, ulti-

mately enabling accurate image classification via fully connected layers [9].

The success of CNNs in various medical imaging domains has spurred interest in their application to breast cancer detection. CNNs have shown potential in analyzing ultrasound images of breast tissue, effectively distinguishing different types of abnormalities. Ultrasound imaging is favored for its safety, non-invasiveness, and cost-effectiveness; however, its manual interpretation poses challenges due to noise and the subtlety of distinguishing features. Integrating CNNs into breast cancer detection workflows can facilitate large-scale screening programs, especially in resource-limited settings. Automated systems powered by CNNs can process vast amounts of imaging data efficiently, reducing the burden on radiologists and enabling timely interventions. As such, the development and refinement of CNN-based models for breast cancer detection represent a crucial step forward in the fight against this pervasive disease.

The structure of this research goes through the following sections. Section 2 discussed the recent research in breast cancer classification. Section 3 presents the typical architecture of Convolutional Neural Networks. While Sections 4 and 5 discuss the utilized breast cancer dataset for the proposed CNN architecture. To demonstrate the accuracy of the proposed architecture, various experiments are conducted and evaluated in Section 6. The main findings of this research, along with some future directions, are discussed in Section 7.

## 2. RELATED WORKS

Many studies have underscored the potential of these advanced methods to enhance both the accuracy and efficiency of diagnoses. Such improvements have been achieved through a diverse array of approaches. For instance, the authors in [24] constructed a Convolutional Neural Network (CNN) model to categorize mammography images into normal, benign, and malignant categories to identify breast cancer cases. The model, trained on preprocessed images, outperformed previous methods with accuracies of 0.8585 and 0.8271, respectively. Falconi et al. [8] reported the first results for using transfer learning to classify breast anomalies as cancers. ResNet50 and MobileNet emerged as the winners among the several deep learning models they tested. A 78.4% and a 74.3% percent accuracy rate, respectively, were the most significant results achieved by the two models.

An innovative method was presented by Ashurov et al. [4] to improve the CNN models' interpretability and robustness in classifying breast cancer histopathology images. This method integrates transfer learning with attention processes. Their approach achieves up to 99.6% test accuracy rates using pre-trained models such as Xception, VGG16, ResNet50, MobileNet, and DenseNet121, enhanced with the convolutional block attention module (CBAM). However, the authors in [10] employed a pre-trained EfficientNet-b0 deep learning model for breast cancer classification with an average accuracy obtained 95.4% and 99.7% for two datasets.

In another study, Rahman et al. [18] present an innovative multi-scale transfer learning model named "BreastMultiNet" for breast image identification. This model combines VGG19 with DenseNet201 to capture low-level properties and construct a multi-scale feature learning process to evaluate these features at various scales. Their architecture, containing 39,013,634 parameters, significantly extends the capacities of DenseNet201 and VGG19 individually. The framework integrates microscopic image sharpening, blurring, texturing, and gradient alignment, achieving remarkable performance improvements.

Additionally, Yao et al. [29] suggested a Deep Neural Network with an Attention Mechanism for Breast Cancer Histology Image Classification that utilizes CNNs and Recurrent Neural Networks. Unlike the conventional serial technique, which involves extracting visual features using a CNN and then feeding them into an RNN, their solution employs a parallel structure consisting of both a CNN and an RNN for feature extraction. To merge the information retrieved by the model's two distinct neural network architectures, they use a unique perceptron attention mechanism borrowed from the natural language processing domain. The model employs switchable normalization instead of general batch normalization in the convolution layer and uses the latest regularization technology, targeted dropout, in the last three fully connected layers. During the testing phase, model fusion and test time augmentation technology are applied on three different datasets of hematoxylin-eosin-stained breast biopsy images. The results demonstrate that their model significantly outperforms state-of-the-art methods.

In [12], the authors proposed an approach that integrates two primary components: transfer learning and convolutional neural networks (CNNs). The hyperparameters of the CNN model were adjusted to improve the classification performance. The results demonstrated that the strategies provided had a substantial positive impact on accuracy across all datasets. Specifically, the combined datasets saw an accuracy improvement of 92.27%, MIAS achieved a 95.95% accuracy, DDSM achieved a 99.39% accuracy, and IN-breast achieved a 96.53% accuracy.

Unlike previous studies that have employed intricate multi-stage frameworks, This research takes a more streamlined approach by leveraging a single-stage convolutional neural network (CNN) architecture. This choice contrasts with the complex methodologies often used in this field, aiming for simplicity and efficiency in accurately classifying breast cancer.

## 3. CONVOLUTIONAL NEURAL NETWORKS

Convolutional Neural Networks are a class of deep learning models with exceptional performance in image recognition tasks. The architecture of CNNs is characterized by distinct layers tailored for handling multidimensional data, making them particularly well-suited for image analysis [25]. According to [11], Figure 2 shows typical CNN architecture.

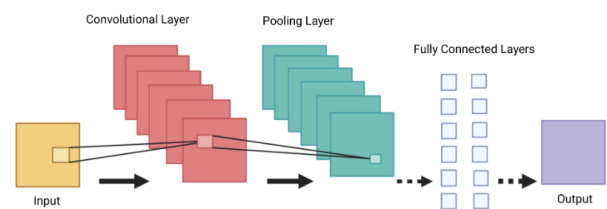


Fig. 2. Typical CNN architecture [11]

The backbone of CNNs is formed by convolutional layers, which apply filters across input images to extract localized features such as edges and textures. These filters are systematically learned during training, enabling the network to detect and emphasize relevant patterns within the data automatically.

Concurrently, pooling layers facilitate spatial downsampling, reducing the dimensionality of feature maps while preserving critical information. This is a pivotal step in managing computational complexity and enhancing the model's robustness.

Central to CNNs' efficacy is their hierarchical feature extraction process. Beginning with raw pixel values, each successive layer refines extracted features through non-linear activation functions like Rectified Linear Units (ReLU). This promotes the network's ability to model complex relationships within data.

The culmination of this process occurs in fully connected layers, where higher-level abstractions are leveraged for accurate classification or regression tasks. This architectural design supports intricate data representations and facilitates the network's generalization capacity across diverse datasets. One common feature of feed-forward neural networks is their complete connectivity, with all neurons in one layer linked to all neurons in the next. Due to their "full connectivity," these networks are predisposed to overfit data. Generally, regularization aims to avoid overfitting by reducing connectivity, punishing parameters during training (e.g., by weight decay), or both.

CNNs stand out from traditional ML algorithms because they can automatically extract features on a massive scale, eliminating the necessity for human feature engineers [30]. Because of the convolutional layers, CNNs can detect and extract features and patterns from data regardless of translation, size, orientation, or position changes.

In addition to image classification tasks, CNNs have many other potential applications, including time series analysis, speech recognition, and natural language processing [26][23][6]. The architectural design of Convolutional Neural Networks supports sophisticated data representations and enables the network to generalize effectively across diverse datasets. This generalization capability is crucial in medical imaging applications, where accurate and consistent diagnosis across different patient cases is essential [3, 28, 16].

#### 4. BREAST CANCER DATASET

The utilized dataset in this study is publicly available from [1]. The dataset is valuable for researchers developing and evaluating machine learning algorithms for breast cancer classification using ultrasound imaging. The dataset [19] encompasses breast ultrasound scans from a diverse group of 600 female patients aged 25 to 75 years old. The dataset boasts a collection of 780 images, all stored in the widely compatible PNG format. Each image has a uniform size of  $500 \times 500$  pixels, ensuring consistency for machine learning algorithms that rely on image dimensions. Significantly, the dataset goes beyond just the raw images. It incorporates crucial ground truth labels for each image, classifying them as normal, benign, or malignant, as shown in Figure 3. This labeled data allows researchers to train and test their algorithms to achieve accurate differentiation between healthy and cancerous tissue.

By providing a comprehensive collection of labeled ultrasound images, this dataset paves the way for advancements in the early detection of breast cancer using automated image analysis techniques.

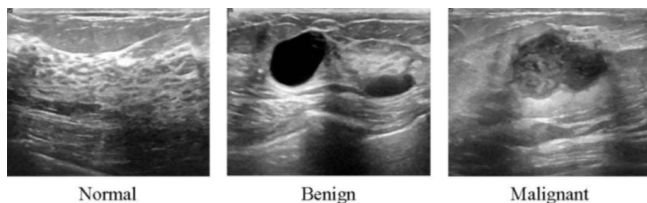


Fig. 3. Sample image of the database [1]

#### 4.1 Preprocessing

In preparation for feeding into the convolutional neural network (CNN) model, a vital preprocessing step: is image resizing employed. The original breast cancer images were scaled to various dimensions, encompassing  $32 \times 32$ ,  $56 \times 56$ ,  $128 \times 128$ , and  $256 \times 256$  pixels while preserving their three color channels (RGB). This resizing ensures compatibility with the CNN's input layer dimensions and fosters computational efficiency during training by reducing the number of pixels the model needs to process.

Additionally, standardizing image sizes helps maintain a uniform scale across all samples, reducing variability arising from differing resolutions. Smaller sizes like  $30 \times 30$  pixels can significantly reduce computational cost and training time. Still, there's a risk of losing crucial details within the image that might be vital for accurate cancer detection. Conversely, larger sizes like  $256 \times 256$  pixels can preserve more detail but may increase training time and resource consumption. Through experimentation, we aim to identify the ideal resize dimension that balances computational efficiency and preserving information necessary for the CNN to effectively distinguish between cancerous and normal tissues.

#### 5. THE PROPOSED CNN

In the fight against breast cancer, early and accurate detection is paramount. CNNs have emerged as powerful tools for analyzing medical images, offering the potential to automate breast cancer screening. However, a critical factor influencing CNN performance is the size of the input image. This study explores the impact of image size by proposing various CNN architectures specifically designed to handle breast cancer images resized to different dimensions, including  $32 \times 32$ ,  $56 \times 56$ ,  $128 \times 128$ , and  $256 \times 256$  pixels, to classify the breast ultrasound images into three categories: malignant, benign, and normal tissues.

The aim is to identify the optimal balance between computational efficiency, feature preservation, and accurate breast cancer classification by investigating CNN structures tailored to each image size. While the core principles of CNNs remain consistent across different image sizes, the specific model structure can be adapted for each variation. The process starts with three convolutional layers that extract hierarchical features from the input images using ReLU activation functions.

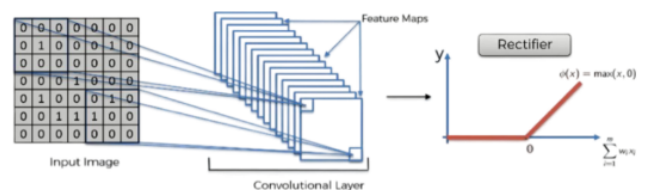


Fig. 4. The impact of ReLU activation function [22]

ReLU can add non-linearity to the model, allowing it to effectively learn intricate relationships between image characteristics and their respective classes, as given in Figure 4.

Each convolutional layer is followed by a max-pooling operation, which reduces the spatial dimensions of the feature maps while retaining essential features, as illustrated in Figure 5. These features are instrumental in achieving precise differentiation among malignant, benign, and normal tissue types.

Post convolution and pooling, a flattening layer transforms the 2D feature maps into a 1D vector, preparing them for input into the

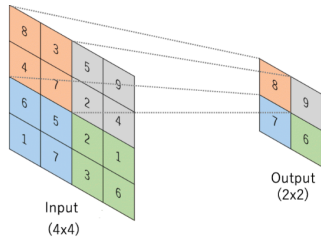


Fig. 5. An illustrative example of Max Pooling [20]

subsequent dense (fully connected) layers. The final dense layer includes Three neurons with softmax activation, generating probabilities for the three classes. Figures 6 and 7 show the whole layers of the proposed CNNs for various image resolutions.

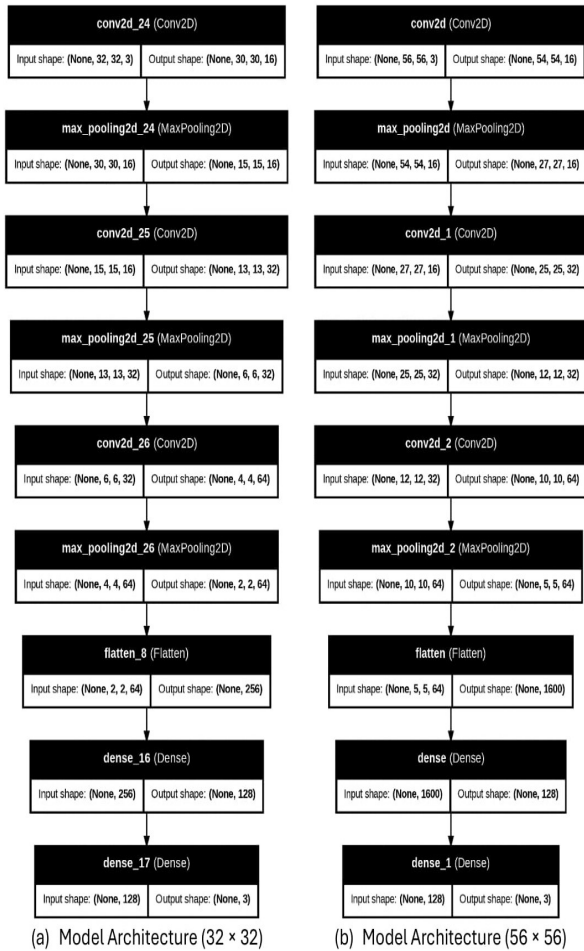


Fig. 6. Proposed CNN for image resolution (32×32) and (56×56)

In figure 6(a), and (b) the three convolutional layers apply filters to the input image to extract features and create feature maps. Following each convolution layer, a max\_pooling layer exists to down-sample the feature maps by taking the maximum value within a specified region. This reduces the dimensionality of the data. A

flattened layer is followed to reshape the feature maps into a one-dimensional vector, preparing the data for the fully connected layers. the fully connected layers combine the extracted features into a fixed-size vector and perform classification. The final dense layer typically has the number of neurons equal to the number of classes in the classification problem. The primary difference between Figure 6 (a) and (b) lies in the input image size. Figure 6 (a) for 32x32 images has a smaller input, leading to fewer neurons in the fully connected layers. Meanwhile, the fully connected layers in Figure 6(b) for 56x56 images have a larger number of neurons, indicating that they can capture more complex patterns from the larger input.

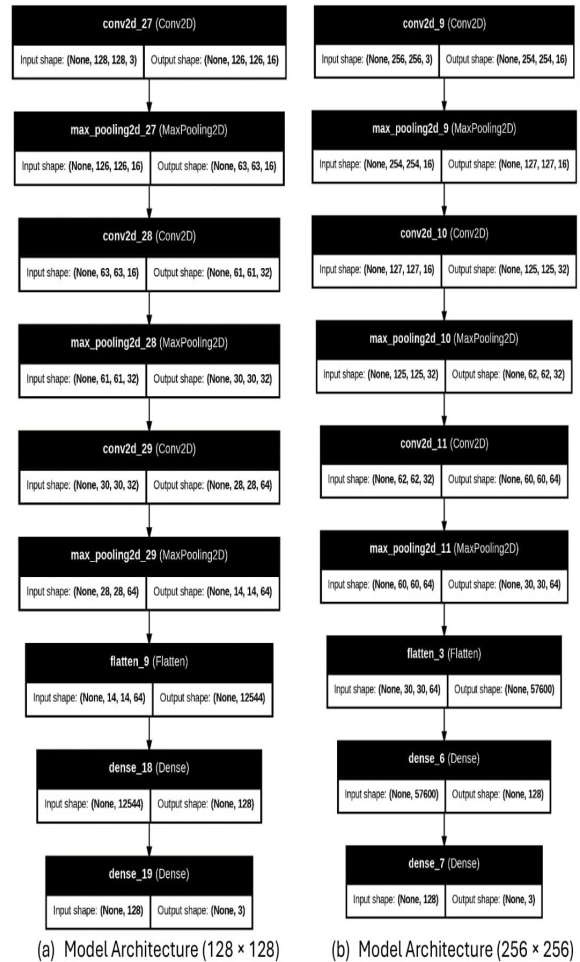


Fig. 7. Proposed CNN for image resolution (128×128) and (256×256)

The same architectures are illustrated in Figure 7 (a) where the input image size is 128×128 and Figure 7 (b) 256×256 pixels as input. The number of channels (3) likely indicates that the images are in RGB format. The final layer produces a vector of size 3, suggesting that the model is designed to classify images into three categories.

Figure 8 shows the overall process of the proposed model that acquires the ability to classify images, utilizing deep learning to improve the accuracy and efficiency of breast cancer diagnosis.

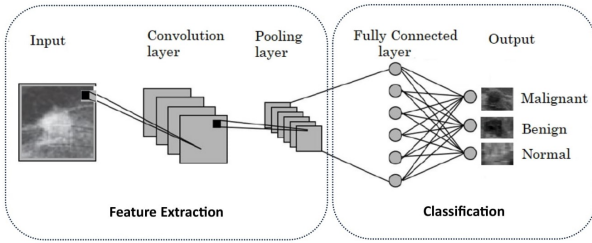


Fig. 8. Proposed CNN for Breast cancer Classification

## 6. EXPERIMENTAL RESULTS

The following section details the experimental results of applying CNN models to the prepared dataset. We evaluated the performance of each model using a suite of metrics, including accuracy, precision, recall, and F1-score. These metrics were calculated for both the training data, used to establish the model, and the testing data, which assessed the model's ability to generalize to unseen data. This analysis allows for a comprehensive comparison of the models' effectiveness in diagnosing breast cancer. Understanding how well our model performs hinges on a foundation of specific terms such as *TP* (i.e., The model's prediction perfectly aligns with the real-world situation, both pointing towards a positive outcome), *TN* (i.e., The predicted negative outcome is verified by the actual negative label.), *FP* (i.e., The model mistakenly identifies an instance as positive, while the ground truth label confirms it as negative), and *FN* (i.e., The model mistakenly classifies an instance as negative, while the ground truth label confirms it as positive). These terms, which act as the building blocks of our evaluation, will be the cornerstone of calculating the metrics that ultimately reveal the model's strengths and weaknesses. A high number of *TP*s and *TN*s indicates good overall accuracy, while a high number of *FP*s and *FN*s suggests the model is making mistakes in its classifications.

—Accuracy: This measure represents the percentage of predictions the model gets correct concerning the total predictions (i.e., *TotalPredictions*). It can be computed as follows.

$$Accuracy = \frac{TP + TN}{TotalPredictions} \quad (1)$$

Accuracy in breast cancer classification reflects the proportion of instances where the model accurately classifies malignant and benign tissue samples.

—Precision (*Pre*): This metric focuses on the positive predictions. It quantifies the ratio of correctly identified positive instances to the total number of positive predictions made by the model. It can be computed as follows.

$$Precision = \frac{TP}{TP + FP} \quad (2)$$

High precision is crucial in breast cancer diagnosis to minimize false positives, which can lead to unnecessary biopsies.

—Recall (*Rec*): It quantifies the percentage of accurately identified positive examples among all real positive examples. It can be computed as follows.

$$Recall = \frac{TP}{TP + FN} \quad (3)$$

High recall is essential to avoid missing true positives, which could lead to delayed treatment.

—F1-Score: This metric is a consolidated indicator of the classifier's efficacy in classifying instances within a specific class. It is calculated as the harmonic mean of accuracy and recall, balancing the model's ability to correctly identify positive cases (recall) and avoid false positives (accuracy), and computed according to the following formula.

$$F1 = 2 \cdot \frac{Pre \cdot Rec}{Pre + Rec} \quad (4)$$

The experimental setup is summarized in Table 1. The model was trained using an Adam optimizer with a batch size of 8, and the model was trained for 30 epochs. The dataset comprised 1030 images categorized into three distinct classes. Table 2 also provides a detailed breakdown of the image distribution across each class.

Table 1. Tuning Set and Testing Set

Hyperparameter	Value
Initial Learning Rate	$1.0000 \times 10^{-4}$
Mini-batch Size	8
Shuffle	Every Epoch
Optimizer	Adam
Max Epochs	30
Execution Environment	CPU

Table 2. Number of Images per Class

Class	Number of Images
Malignant	360
Benign	537
Normal	133
Training Samples	(80%)
Testing Samples	(20%)

### 6.1 Performance Analysis

The evaluation results of training CNNs on image datasets with varying resolutions are listed in Table 3 and in testing data.

From analyzing the results in Table 3, the overall accuracy increases with image resolution, reaching a peak at  $256 \times 256$  (0.998) for training data and (0.834) for testing data. Here is a positive correlation between the amount of image detail and model accuracy, at least up to a certain point.

Like accuracy, precision and recall generally increase with resolution, reaching a peak at  $256 \times 256$  for training and testing data. This indicates that the model better identifies the correct class (positive or negative) with more detailed images. With image resolution  $256 \times 256$ , the model's accuracy is improved by 0.486% when compared with resolutions  $(32 \times 32$  and  $56 \times 56)$  and improved by 0.122% compared with resolution  $128 \times 128$  in the training. The performance metrics (accuracy and recall) for  $32 \times 32$  and  $256 \times 256$  on the testing set are similar. This might indicate an optimal resolution range for this specific model and dataset. However, the jump in accuracy from  $56 \times 56$  to  $128 \times 128$  is more significant than the increase from  $128 \times 128$  to  $256 \times 256$ . This suggests that the model benefits more from increased resolution up to a certain point.

Table 3. Performance Metrics for Different Resolutions

Dataset	Resolution	Accuracy	Precision	Recall	F1 Score
Training	32×32	0.993932039	0.993952897	0.993932039	0.993926701
	56×56	0.993932039	0.993951490	0.993932039	0.993934030
	128×128	0.997572816	0.997572816	0.997572816	0.997572816
	256×256	0.9987864078	0.9987892235	0.9987864078	0.9987860572
Testing	32×32	0.834951456	0.840674499	0.834951456	0.834865186
	56×56	0.766990291	0.786603573	0.766990291	0.767328614
	128×128	0.815533981	0.813782581	0.815533981	0.813986476
	256×256	0.834951456	0.834370435	0.834951456	0.834098435

## 6.2 Confusion Matrix

Furthermore, the confusion matrix can provide a class-by-class breakdown of the classifier’s effectiveness. This breakdown includes the counts of true positives, false positives, true negatives, and erroneously listed false positives. Figures 9, 10, 11, and 12 show the confusion matrices of CNN with various image resolutions in training and testing data.

According to Figure 9, the model exhibits exceptionally high accuracy, with almost all instances correctly classified. This is evident in the large diagonal values (true positives) and low off-diagonal values (errors) regarding training. Specifically, the model correctly classified 819 cases out of 824 (99.93%) in training and 172 out of 206 (83.49%) in testing. From the testing confusion matrix, the model correctly identifies a majority of malignant cases (56 out of 72), but there are 15 false positives (predicted as benign) and 1 false negative (predicted as normal). The model performs well in classifying benign cases for the Benign class, with 96 correct predictions out of 107. However, there are 4 false negatives (predicted as malignant) and 7 false positives (predicted as normal). The model performs reasonably well classifying normal cases, with 20 correct predictions out of 27. However, there are 6 false positives (predicted as benign) and 1 false negative (predicted as malignant).

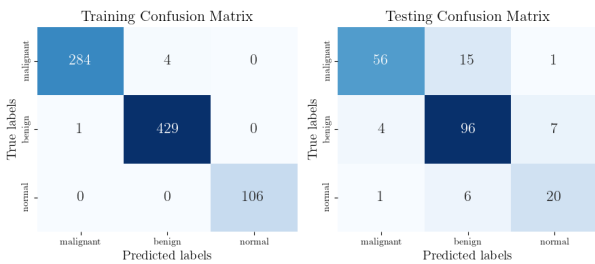


Fig. 9. Confusion matrix for image resolution of (32×32)

For image resolution 56×56 in the training case, the CNN model correctly identifies almost all malignant cases, indicating good sensitivity for this class. Similar to malignant, the model performs exceptionally well in classifying benign cases except only for 3 cases. The model accurately classified 105 cases out of 106 for the normal class. In the case of testing, the CNN diagnosis model has achieved a reasonable performance in classifying normal cases, with 18 correct predictions out of 27. However, there are 2 false positives (predicted as benign) and 7 false negatives (predicted as malignant). For the other two classes (Malignant and Benign), the model accurately identifies 65 out of 72 malignant cases but has 3 false positives, 4 false negatives, and 75 correct predictions for benign cases.

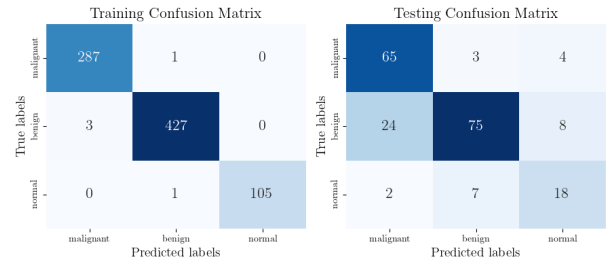


Fig. 10. Confusion matrix for image resolution of (56×56)

Figure 11 presents the confusion matrices for breast cancer diagnosis using 128×128 image resolution, separately for training and testing datasets. In the training confusion matrix, the model correctly classified almost all instances (99.75%), with very few misclassifications (0.24%). However, in the testing data, the model correctly identifies a majority of malignant cases (59 out of 72), but there are 11 false positives (predicted as benign) and 2 false negatives (predicted as normal). In contrast, the model achieves 92 correct predictions out of 107 correct predictions when classifying Benign cases and 17 correct predictions out of 27 when classifying normal cases.

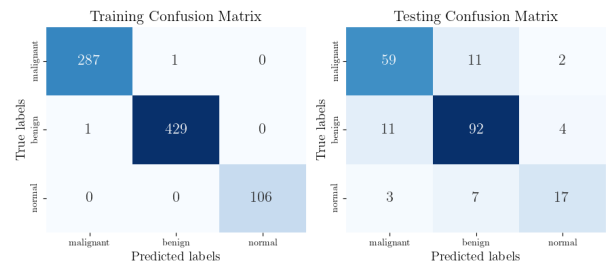


Fig. 11. Confusion matrix for image resolution of (128×128)

Increasing image resolution to 256x256 could enhance the classification accuracy, providing the model with more detailed information for distinguishing between various classes, as shown in Figure 12. The CNN model correctly classified 823 out of 824 cases as true positive and true negative in training data while misclassified 34 out of 206 cases as false positive and false negative in testing data. Overall, good performance for Benign and Malignant classes: The model performs well in classifying benign and malignant cases, with high accuracy and few misclassifications. By which 64 malignant cases were correctly identified as malignant (16.50%), 90 benign cases were correctly identified as benign (43.68%), and 18

normal cases were correctly identified as normal (8.73%) out of 206 test cases.

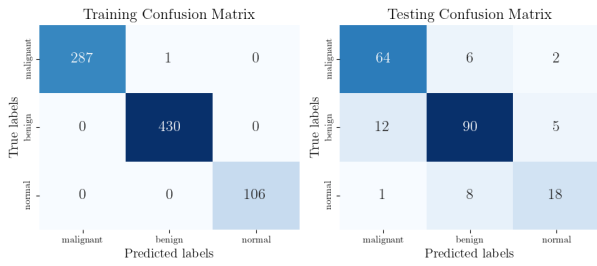


Fig. 12. Confusion matrix for image resolution of (256x256)

### 6.3 Convergence Curves

Moreover, accuracy and loss curves are essential tools for evaluating the performance of a DL model during training. The accuracy curve illustrates how well the model predicts correct outcomes over time, ideally increasing as training progresses. Conversely, the loss curve depicts the model's error rate (i.e., the discrepancy between the model's predicted outputs and the actual ground truth labels for training data), decreasing as the model learns from the data. Figures 13, 14, 15, and 16 show the accuracy and loss curves for 32x32, 56x56, 128x128, and 256x256, respectively.

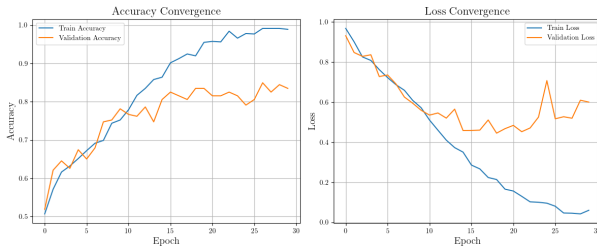


Fig. 13. Accuracy and Loss convergence curves for image resolution of (32x32)

From Figure 13, the training accuracy curve shows a consistent upward trend, indicating that the model effectively learns from the training data. While the training accuracy continues to rise, the validation accuracy plateaus around epoch 20. Regarding the loss convergence, both training and validation loss curves show a downward trend, indicating that the model minimizes its errors over time.

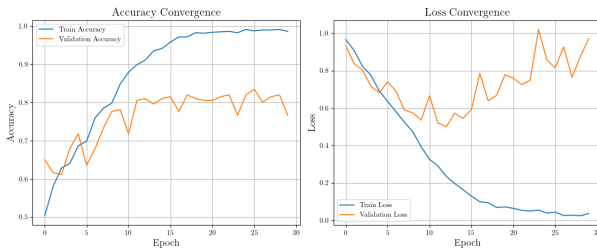


Fig. 14. Accuracy and Loss convergence curves for image resolution of (56x56)

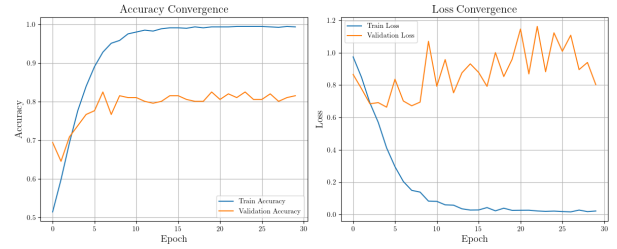


Fig. 15. Accuracy and Loss convergence curves for image resolution of (128x128)

For image resolutions 56x56 and 128x128, both training and validation accuracy curves have achieved steady improvement. In contrast, the loss curves exhibit some oscillations, particularly in the validation loss, due to the limitations of data classes.

The accuracy curve in Figure 16 shows a rapid initial improvement, indicating effective learning from the training data. The training and validation loss curves consistently decline, suggesting that the model progressively reduces error. Generally, lower loss values indicate that the model's predictions are close to the true values, signifying better performance. A higher accuracy value means the model has made more correct predictions, which is desirable.

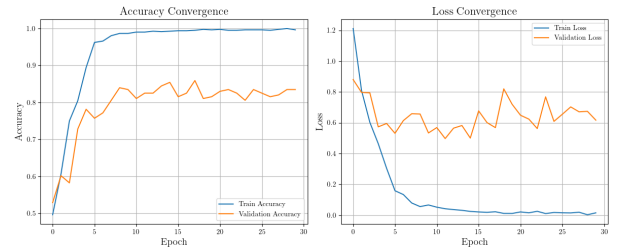


Fig. 16. Accuracy and Loss convergence curves for image resolution of (256x256)

## 7. CONCLUSION

In conclusion, breast cancer poses a significant global health challenge, affecting millions annually with varying severity and outcomes. Early detection and diagnosis remain pivotal in enhancing survival rates and treatment efficacy, yet existing methods face interpretational challenges and potential diagnostic inaccuracies. Leveraging recent advancements in deep learning, this study introduced a tailored convolutional neural network (CNN) architecture for classifying breast ultrasound images into malignant, benign, and normal tissues. The proposed CNN model demonstrated notable accuracy, precision, recall, and F1-score metrics improvements through rigorous experimentation on various image resolutions. These findings underscore the potential of CNNs in revolutionizing breast cancer detection by providing more accurate and efficient diagnostic tools. By automating image analysis and reducing dependency on manual interpretation, CNN-based systems can significantly alleviate the burden on medical professionals, paving the way for enhanced patient care and outcomes in the fight against breast cancer. For future work, one potential direction is to explore the integration of other imaging modalities, such as mammography and MRI as well as utilizing various DL models.

## 8. REFERENCES

- [1] W. Al-Dhabyani, M. Gomaa, H. Khaled, and A. Fahmy. Dataset of breast ultrasound images. *Data in Brief*, 28:104863, Feb 2020.
- [2] Laha Ale, Alaa Sheta, Longzhuang Li, Ye Wang, and Ning Zhang. Deep learning based plant disease detection for smart agriculture. In *2019 IEEE Globecom Workshops (GC Wkshps)*, pages 1–6, 2019.
- [3] Laith Alzubaidi, Jinglan Zhang, Amjad J. Humaidi, Ayad Al-Dujaili, Ye Duan, Omran Al-Shamma, José I. Santamaría, Mohammed Abdulraheem Fadhel, Muthana Al-Amidie, and Laith Farhan. Review of deep learning: concepts, cnn architectures, challenges, applications, future directions. *Journal of Big Data*, 8, 2021.
- [4] Asadulla Ashurov, Samia Allaoua Chelloug, Alexey Tselykh, Mohammed Saleh Ali Muthanna, Ammar Muthanna, and Mehdhar S. A. M. Al-Gaashani. Improved breast cancer classification through combining transfer learning and attention mechanism. *Life*, 13(9), 2023.
- [5] Benjamin Byers and Alaa Sheta. Design of convolutional neural networks for fish recognition and tracking. *Artificial Intelligence and Machine Learning AIML*, 22(1):1–9, 5 2022.
- [6] Nagajyothi Dimmita and P. Siddaiah. Speech recognition using convolutional neural networks. *International Journal of Engineering and Technology(UAE)*, 7:133–137, 09 2018.
- [7] Elizabeth Endri, Alaa Sheta, and Hamza Turabieh. Road damage detection utilizing convolution neural network and principal component analysis. *International Journal of Advanced Computer Science and Applications*, 11(6), 2020.
- [8] Lenin G. Falconí, María Pérez, and Wilbert G. Aguilar. Transfer learning in breast mammogram abnormalities classification with mobilenet and nasnet. In *2019 International Conference on Systems, Signals and Image Processing (IWSSIP)*, pages 109–114, 2019.
- [9] Ian Goodfellow, Yoshua Bengio, and Aaron Courville. *Deep Learning*. MIT Press, 2016. <http://www.deeplearningbook.org>.
- [10] K Jabeen, M A Khan, J Balili, M Alhaisoni, N A Almujaally, H Alrashidi, U Tariq, and J H Cha. Bc2netrf: Breast cancer classification from mammogram images using enhanced deep learning features and equilibrium-jaya controlled regula falsi-based features selection. *Diagnostics (Basel, Switzerland)*, 13(7):1238, 2023.
- [11] Loucia Karatzia, Nay Aung, and Dunja Aksentijevic. Artificial intelligence in cardiology: Hope for the future and power for the present. *Frontiers in Cardiovascular Medicine*, 9, 10 2022.
- [12] R. Karthiga, K. Narasimhan, and Rengarajan Amirtharajan. Diagnosis of breast cancer for modern mammography using artificial intelligence. *Mathematics and Computers in Simulation*, 202:316–330, 2022.
- [13] Yann LeCun, Y. Bengio, and Geoffrey Hinton. Deep learning. *Nature*, 521:436–44, 05 2015.
- [14] Geert Litjens, Thijs Kooi, Babak Ehteshami Bejnordi, Arnaud Arindra Adiyoso Setio, Francesco Ciompi, Mohsen Ghahfoorian, Jeroen A.W.M. van der Laak, Bram van Ginneken, and Clara I. Sánchez. A survey on deep learning in medical image analysis. *Medical Image Analysis*, 42:60–88, 2017.
- [15] Market.us. Breast cancer market analysis, size, trends and forecast to 2032, 2024. Accessed: 2024-08-07.
- [16] Keiron O’Shea and Ryan Nash. An introduction to convolutional neural networks. *CoRR*, abs/1511.08458, 2015.
- [17] Aisha Patel. Benign vs Malignant Tumors. *JAMA Oncology*, 6(9):1488–1488, 09 2020.
- [18] Md. Mahbubur Rahman, Md. Saikat Islam Khan, and Hafiz Md. Hasan Babu. Breastmultinet: A multi-scale feature fusion method using deep neural network to detect breast cancer. *Array*, 16:100256, 2022.
- [19] Paulo Sergio Rodrigues. Breast ultrasound image. Mendeley Data, 2017.
- [20] Md Motiur Rahman Sagar and Martin Dyrba. Learning shape features and abstractions in 3d convolutional neural networks for detecting alzheimer’s disease, 2020.
- [21] Alaa Sheta, Hamza Turabieh, Sultan Aljahdali, and Abdulaziz Alangari. Pavement crack detection using convolutional neural network. In Gordon Lee and Ying Jin, editors, *Proceedings of 35th International Conference on Computers and Their Applications*, volume 69 of *EPiC Series in Computing*, pages 214–223. EasyChair, 2020.
- [22] SuperDataScience. The ultimate guide to convolutional neural networks (cnn). *SuperDataScience Blog*, august 2023.
- [23] A. Taherkhani, G. Cosma, and T.M. McGinnity. A deep convolutional neural network for time series classification with intermediate targets. *SN Computer Science*, 4(1):832, 2023.
- [24] Y. J. Tan, Kok-Swee Sim, and Fung Fung Ting. Breast cancer detection using convolutional neural networks for mammogram imaging system. *2017 International Conference on Robotics, Automation and Sciences (ICORAS)*, pages 1–5, 2017.
- [25] Maria Vakalopoulou, Stergios Christodoulidis, Ninon Burgos, Olivier Colliot, and Vincent Lepetit. *Deep Learning: Basics and Convolutional Neural Networks (CNNs)*, pages 77–115. Springer US, New York, NY, 2023.
- [26] Wei Wang and Jianxun Gang. Application of convolutional neural network in natural language processing. In *2018 International Conference on Information Systems and Computer Aided Education (ICISCAE)*, pages 64–70, 2018.
- [27] World Health Organization. Breast cancer: Prevention and control, 2024. Accessed: 2024-08-07.
- [28] Rikiya Yamashita, Mizuho Nishio, Richard Do, and Kaori Togashi. Convolutional neural networks: an overview and application in radiology. *Insights into Imaging*, 9, 06 2018.
- [29] Hongdou Yao, Xuejie Zhang, Xiaobing Zhou, and Shengyan Liu. Parallel structure deep neural network using cnn and rnn with an attention mechanism for breast cancer histology image classification. *Cancers*, 11:1901, 11 2019.
- [30] X. Zhao, L. Wang, and Y. et al. Zhang. A review of convolutional neural networks in computer vision. *Artificial Intelligence Review*, 57(99), 2024.